

This article was downloaded by:

On: 25 January 2011

Access details: *Access Details: Free Access*

Publisher *Taylor & Francis*

Informa Ltd Registered in England and Wales Registered Number: 1072954 Registered office: Mortimer House, 37-41 Mortimer Street, London W1T 3JH, UK



## Separation Science and Technology

Publication details, including instructions for authors and subscription information:

<http://www.informaworld.com/smpp/title~content=t713708471>

### Electrodialysis of Vanadium(III) and Iron(II) Ions from a Simulated Decontamination Solution

Joon-Bo Shim<sup>a</sup>; Won-Zin Oh<sup>a</sup>; Byung-Jik Lee<sup>a</sup>; Hyun-Soo Park<sup>a</sup>; Jong-Duk Kim<sup>b</sup>

<sup>a</sup> KOREA ATOMIC ENERGY RESEARCH INSTITUTE, YUSONG-GU, TAEJON, SOUTH KOREA

<sup>b</sup> DEPARTMENT OF CHEMICAL ENGINEERING, KOREA ADVANCED INSTITUTE OF SCIENCE AND TECHNOLOGY, YUSONG-GU, TAEJON, SOUTH KOREA

Online publication date: 07 December 1999

**To cite this Article** Shim, Joon-Bo , Oh, Won-Zin , Lee, Byung-Jik , Park, Hyun-Soo and Kim, Jong-Duk(1999) 'Electrodialysis of Vanadium(III) and Iron(II) Ions from a Simulated Decontamination Solution', *Separation Science and Technology*, 34: 10, 1963 — 1979

**To link to this Article:** DOI: 10.1081/SS-100100749

URL: <http://dx.doi.org/10.1081/SS-100100749>

## PLEASE SCROLL DOWN FOR ARTICLE

Full terms and conditions of use: <http://www.informaworld.com/terms-and-conditions-of-access.pdf>

This article may be used for research, teaching and private study purposes. Any substantial or systematic reproduction, re-distribution, re-selling, loan or sub-licensing, systematic supply or distribution in any form to anyone is expressly forbidden.

The publisher does not give any warranty express or implied or make any representation that the contents will be complete or accurate or up to date. The accuracy of any instructions, formulae and drug doses should be independently verified with primary sources. The publisher shall not be liable for any loss, actions, claims, proceedings, demand or costs or damages whatsoever or howsoever caused arising directly or indirectly in connection with or arising out of the use of this material.

## Electrodialysis of Vanadium(III) and Iron(II) Ions from a Simulated Decontamination Solution

JOON-BO SHIM, WON-ZIN OH, BYUNG-JIK LEE, and HYUN-SOO PARK

NUCLEAR FUEL CYCLE DEVELOPMENT  
KOREA ATOMIC ENERGY RESEARCH INSTITUTE  
P.O. BOX 105, YUSONG-GU, TAEJON, 305-600, SOUTH KOREA

JONG-DUK KIM\*

DEPARTMENT OF CHEMICAL ENGINEERING  
KOREA ADVANCED INSTITUTE OF SCIENCE AND TECHNOLOGY  
373-1, KUSONG-DONG, YUSONG-GU, TAEJON, 305-701, SOUTH KOREA

### ABSTRACT

The transport of vanadium(III) and iron(II) ions through the Nafion 117 cation-exchange membrane in the presence of picolinic acid was investigated by simulating the equilibrium distribution of ionic species as a function of pH, and by electrodialyzing the simulated waste solution. From distribution calculations of the model reaction systems it could be predicted that at pH 1.6 most vanadium ions exist predominantly in the form of the  $V^{III}(Pic^-)_2^+$  complex, and this form of complex permeates across the cation-exchange membrane during electrodialysis. The experimental results, including variations in the color and cation concentrations of the catholyte, confirm the existence of the vanadium(III) picolinate complex. Iron ions permeated into the catholyte were converted to their hydroxide precipitates, which could be formed at the high pH condition resulting from the reduction of hydrogen ions and the production of  $OH^-$  ions by water electrolysis at the cathode. It was also found that the in-situ precipitation of iron in the electrodialyzer could be self-modulated by shifting the catholyte pH from the acidic state to the alkaline state during electrodialysis operation.

**Key Words.** Electrodialysis; Ion-exchange membrane; Nafion; Chemical decontamination; Decontamination waste; Vanadium; Vanadium picolinate complex

\* To whom correspondence should be addressed.

## INTRODUCTION

Electrodialysis (ED) using ion-exchange membranes has been widely used in desalination and concentration of seawater, the removal or recovery of heavy metal ions and hazardous compounds in wastewater, and the separation of amino acids and proteins (1–6). In this process, ionic migration through an ion-exchange membrane takes place when a potential gradient is applied across the membrane; electrostatic interaction within the matrix plays a key role in the transfer of ions. For a cation-exchange membrane, therefore, negatively charged sulfonate groups inhibit the transfer of negatively charged anions (co-ions).

A new technology, named the electrodeionization (EDI) process, has been developed as a means of producing high purity water by combining ion-exchange membranes, resins, and electric current (7). This process uses the alternate cell which consists of ion-permeable membranes and ion-exchange resin beads to capture temporarily feedwater impurities, such as  $\text{Na}^+$  and  $\text{Cl}^-$  ions, etc., and then to make these ions migrate toward the electrodes under the electric field.

Diffusion and permeation of simple salts through ionic polymer matrices can be explained by the ionic interaction between a simple ion and a charged group in a polymer chain. Xue et al. (8) investigated the effects of complexation on ion transport selectivity of Nafion 117 membranes in the gold– and silver–thiourea–water systems, and concluded that the transport rate of ions was significantly reduced by the formation of silver–thiourea complexes. With the same resin, they also studied the sorption of thiourea and the exchange of sodium and silver ions (9). As a result, it was concluded that both the sorption on the Ag-form of the resin and the transport rate of ions can be attributed to the strong interactions between silver–thiourea complexes and sulfonate groups in the membrane.

On the other hand, during in-service inspection and repair work in a nuclear power plant (NPP), occupational radiation exposure can be reduced by introducing dilute chemical decontamination processes. Mixtures of decontamination reagents are used to remove such radioactive contaminants as Co-60 and Co-58 from the inner surface of the NPP primary coolant system. Such radioactive decontamination liquid wastes have been treated by using ion-exchange resin columns. At present, one widely used process is the LOMI (low oxidation-state metal ion) decontamination process (10). However, the process generates large volumes of spent resins (11, 12) to be disposed of after solidification with cement (13, 14). In general, such solidified wastes contain undesirable chelating agents which have the potential to give rise to the migration of radionuclides in geologic media (15). Therefore, reduction of waste volume and the chelating ligands content in the waste is extremely important from the standpoint of waste management.

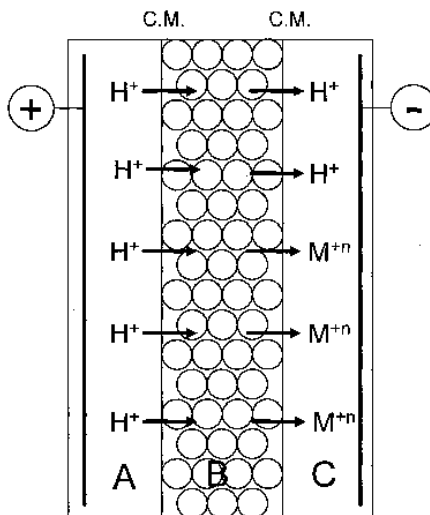


Recently, an electrodialyzer filled with ion-exchange resin beads between two cation-exchange membranes was introduced, and decontamination chemicals in the liquid waste resulting from the LOMI process, such as picolinate, could be recovered by removing cations (16, 17). We believe this resin-filled electrodialyzer would be an attractive and useful device in the field of separation. However, the transport behaviors of cationic species in the resin-filled electrodialyzer have rarely been reported up to now.

In this study we report the transport of cationic species in a resin-filled electrodialyzer. The simulated decontamination waste solution used as a feed contained vanadium(III) and iron(II) picolinate complexes. We have evaluated the equilibrium distribution of these ionic species at different pH values and clarified the permeation behavior of vanadium(III) ion across the cation-exchange membrane in the presence of picolinic acid.

### THE RESIN-FILLED ELECTRODIALYZER

Figure 1 shows a schematic diagram of the resin-filled electrodialyzer including the transport of ionic species. The electrodialyzer cell consists of three compartments separated by two Nafion membranes. The resin beads were filled in the central zone (B). The anode and the cathode were in Zones A and C, respectively. A constant electrical current flows by the migration of positively charged ionic species across the resin bed (B) during electrodialytic operation.



\* C.M. : Cation Exchange Membrane

FIG. 1 Schematic diagram of the resin-filled electrodialyzer and the permeation of ionic species.

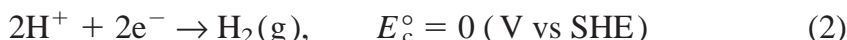


## Electrode Reactions

In an acidic medium, hydrogen ions are produced at the surface of the platinum anode by the electrolysis of water. The hydrogen ions are transferred from the anode compartment (A) to the resin bed (B) and partly to the cathode compartment (C). The dissociation of water at the anode is given by (18, 19).



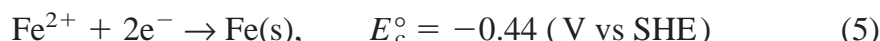
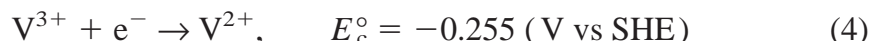
In an acidic catholyte, hydrogen gas is generated from the reduction of  $\text{H}^+$  ions at the cathode (18, 19):



In neutral or alkaline catholyte, however,  $\text{OH}^-$  ions and hydrogen gas are generated from the electrolysis of water (18, 19):



Further, the permeated metal ions can be electrolytically reduced at the cathode surface (19):



## Reactions in the Ion-Exchange Resin Bed

The waste solution fed to the resin bed contains various kinds of metal ions and the chelating agent. The LOMI decontamination process uses a mixture of vanadous formate and picolinic acid, and the active decontamination reagent is vanadium(II) tris picolinate,  $\text{V}(\text{II})(\text{Pic})_3^-$ . One mole of vanadous ion reacts with one mole of ferric ion in the oxide matrix, and vanadous ion reduces ferric ion to ferrous ion. Therefore, ferrous ions are released from the oxide matrix into the bulk solution. As a result, various chemical species, such as  $\text{H}^+$ ,  $\text{OH}^-$ ,  $\text{Na}^+$ ,  $\text{HCOOH}$ ,  $\text{HCOO}^-$ ,  $\text{HPic}$ ,  $\text{Pic}^-$ ,  $\text{V}^{2+}$ ,  $\text{V}^{3+}$ , and  $\text{Fe}^{2+}$ , including metal–picolinate complexes such as  $\text{V}(\text{II})(\text{Pic})_1^+$ ,  $\text{V}(\text{II})(\text{Pic})_2$ ,  $\text{V}(\text{II})(\text{Pic})_3^-$ ,  $\text{V}(\text{III})(\text{Pic})_1^{2+}$ ,  $\text{V}(\text{III})(\text{Pic})_2^+$ ,  $\text{V}(\text{III})(\text{Pic})_3$ ,  $\text{V}(\text{III})(\text{OH})(\text{Pic})_2$ ,  $\text{Fe}(\text{II})(\text{Pic})_1^+$ ,  $\text{Fe}(\text{II})(\text{Pic})_2$ , and  $\text{Fe}(\text{II})(\text{Pic})_3^-$ , are formed in the LOMI decontamination solution (10). Here,  $\text{HPic}$  and  $\text{Pic}^-$  are abbreviations of picolinic acid and picolinate, respectively. The detailed reaction steps are complicated and are not resolved.

For the feed stock in this study, vanadium(III) ions and ferrous ions were mixed with picolinic and formic acids solution at pH 4.5. The expected reactions in the simulated decontamination solution are summarized in Table 1.



TABLE 1  
The Dissociation Equilibria and  $pK_a$  Values (20-23)

Dissociation reactions	$pK_a$
$\text{HPic} \rightleftharpoons \text{H}^+ + \text{Pic}^-$	5.21
$\text{V(III)(Pic)}_1^{2+} \rightleftharpoons \text{V}^{3+} + \text{Pic}^-$	5.72
$\text{V(III)(Pic)}_2^+ \rightleftharpoons \text{V(III)(Pic)}_1^{2+} + \text{Pic}^-$	6.56
$\text{V(III)(Pic)}_3 \rightleftharpoons \text{V(III)(Pic)}_2^+ + \text{Pic}^-$	4.07
$\text{V(III)(OH)(Pic)}_3 + \text{H}^+ \rightleftharpoons \text{V(III)(Pic)}_2^+ + \text{Pic}^-$	2.66
$\text{Fe(II)(Pic)}_1^+ \rightleftharpoons \text{Fe}^{2+} + \text{Pic}^-$	4.90
$\text{Fe(II)(Pic)}_2 \rightleftharpoons \text{Fe(II)(Pic)}_1^+ + \text{Pic}^-$	4.10
$\text{Fe(II)(Pic)}_3^- \rightleftharpoons \text{Fe(II)(Pic)}_2 + \text{Pic}^-$	3.30

## EXPERIMENTAL

### Chemicals and Materials

The simulated LOMI decontamination waste solution was prepared with chemicals, and used as a feed. The feed concentrations of V(III) and Fe(II) were 6 and 4.8 mM, respectively. The molar ratio of vanadium:picolinic acid:formic acid in a feed was 1:3:10. The solution pH was adjusted to 4.5 by adding NaOH. The sodium concentration in the simulated waste solution was about 81.3 mM. Such chemicals as  $\text{VCl}_3$  (Aldrich Chemical Co., GR),  $\text{FeSO}_4$  (Fischer Scientific Co., GR), NaOH (Ducksan Pharmaceutical Co., GR),  $\text{HCOOH}$  (Yakuri Pure Chemical Co., GR) and picolinic acid (Tokyo Chemical Co., GR) were used without further purification. The ultrapure water used was produced by passing distilled water through the purification unit (NANOpure-II, Barnstead Co.). The specific resistivity of water was 17.6  $\text{M}\Omega\text{-cm}$ . The cation-exchange resin was  $\text{H}^+$ -form, IRN-77 (Rohm & Haas Co. Ltd., nuclear grade) and the cation-exchange membrane was Nafion 117 ( $\text{H}^+$ -form) manufactured by DuPont Co. Ltd.

### Experimental Apparatus and Procedure

A schematic diagram of the experimental apparatus is shown in Fig. 2. Anolyte and catholyte were 1 N  $\text{H}_2\text{SO}_4$  solutions. 200-mL volumes of electrode solutions were stirred magnetically in the Pyrex glass Erlenmeyer flasks, and recirculated at a flow rate of 70 mL/min through each electrode compartment. The simulated LOMI decontamination waste solution was passed upward at a constant flow rate through the midcompartment of the electrodialyzer. The pH values of the effluent and catholyte discharged from the electrodialyzer were continuously monitored by means of on-line pH elec-



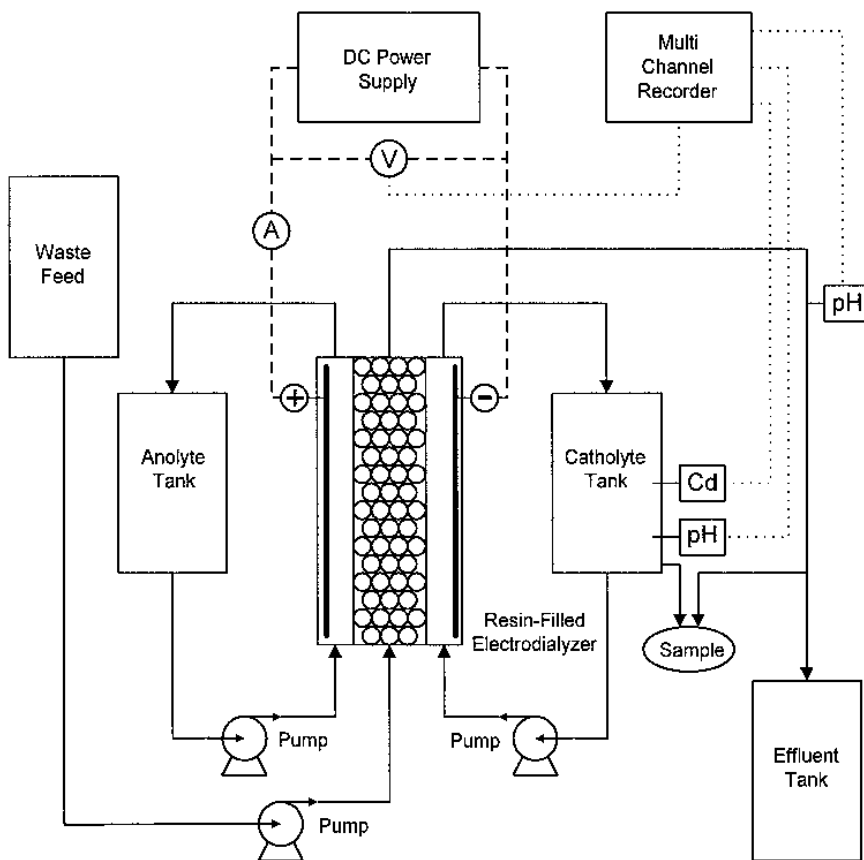


FIG. 2 Schematic diagram of experimental apparatus for electrodialysis of the simulated de-contamination solution.

trodes and the strip chart recorder. After a dc power supply (HPS-305DG, Hanil Electric Co.) was connected to the electrodes, current flowed under the galvanostatic condition and the cell voltage was measured with an electrometer (Model 617, Keithley Co. Ltd.), which has high internal resistance ( $2 \times 10^{14}$  ohm), and also monitored on the recorder.

The resin-filled electrodialyzer was composed of three compartments which were divided by two Nafion 117 cation-exchange membranes. The midcompartment between two membranes was filled with the  $H^+$ -form cation-exchange resin beads. Specifications of the resin-filled electrodialyzer are listed in Table 2. The anode was a platinum plate and the cathode was a type 304 stainless steel plate. The effective areas of the cation-exchange membrane and the electrode were  $20 \text{ cm}^2$  ( $1 \text{ cm W} \times 20 \text{ cm L}$ ). The thickness of each compartment of the electrodialyzer was maintained at 2 mm by using silicon rubber plate gaskets which prevented the leakage of solutions between compartments. The electrodialyzer was fabricated in the filter press type.



TABLE 2  
Main Specifications of the Resin-Filled Electrodialyzer

Items	Specification
Type	Three-compartment cell
Midcompartment thickness, cm	0.2
Effective area of membrane, $\text{cm}^2$	20 [width (1 cm) $\times$ length (20 cm)]
Electrode area, $\text{cm}^2$	20
Construction materials:	
Guard frame	PTFE plate
Membrane	Nafion 117 ( $\text{H}^+$ – form)
Spacer	Woven PE screen
Gasket	Silicone rubber
Anode	Platinum plate
Cathode	S.S. 304 plate

Therefore, each solution in the three compartments could be passed independently. Sheet-flow type spacers made of a woven polyethylene screen were inserted in each electrode compartment to prevent shorting by direct contact between the membranes and the electrodes, and to promote mass transfer at the surface of the membranes and the electrodes.

The resin beads and the membranes were pretreated for 24 hours by soaking in 1 N sulfuric acid solution. The surfaces of the anode and the cathode were polished by using fine sandpaper and emery cloth with an alumina powder suspension. After removing organic materials from the surface with acetone, the electrode surfaces were rinsed with demineralized water.

The electrical conductivity of the catholyte was measured continuously. For every experimental set the cation-exchange membranes and the resin beads were replaced with pretreated fresh ones. Samples of 10 mL effluent and 0.5 mL catholyte were taken at time intervals. The sodium concentration was analyzed by using an Atomic Absorption Spectrophotometer (Model 1100B, Perkin-Elmer Co. Ltd.), and the vanadium and iron concentrations were determined with an Inductively Coupled Plasma Atomic Emission Spectrometer, ICP (Model JY 50P, Jobin Yvon Co. Ltd.).

## RESULTS AND DISCUSSION

### Distribution of Ionic Species in the Ligand Mixture

For the effective separation of the cations from the spent LOMI decontamination solution, information about the complex equilibria of ions in the solution is required. At the equilibrium state the distribution of complexes can be



calculated by the total concentrations of metal ions and ligands, and the pHs of the solutions. For the simulated waste solution used in this study, the chemical equilibria listed in Table 1 were assumed and  $pK_a$  values were obtained from the literature (20–23). The calculations are fairly complicated, but application of the computer programs developed by Perrin and Sayce (24) and by Ingri et al. (25) are particularly useful. Figures 3 and 4 are simulation results which show the different distributions of vanadium(III)–picolinate and iron(II)–picolinate complexes at different molar ratios of the metal to the ligand, respectively.

Figure 4 shows that most of vanadium ions at the inlet of the resin bed exist in the form of the neutral  $V(III)(Pic)_2(OH)$  complex, and ferrous ions pre-

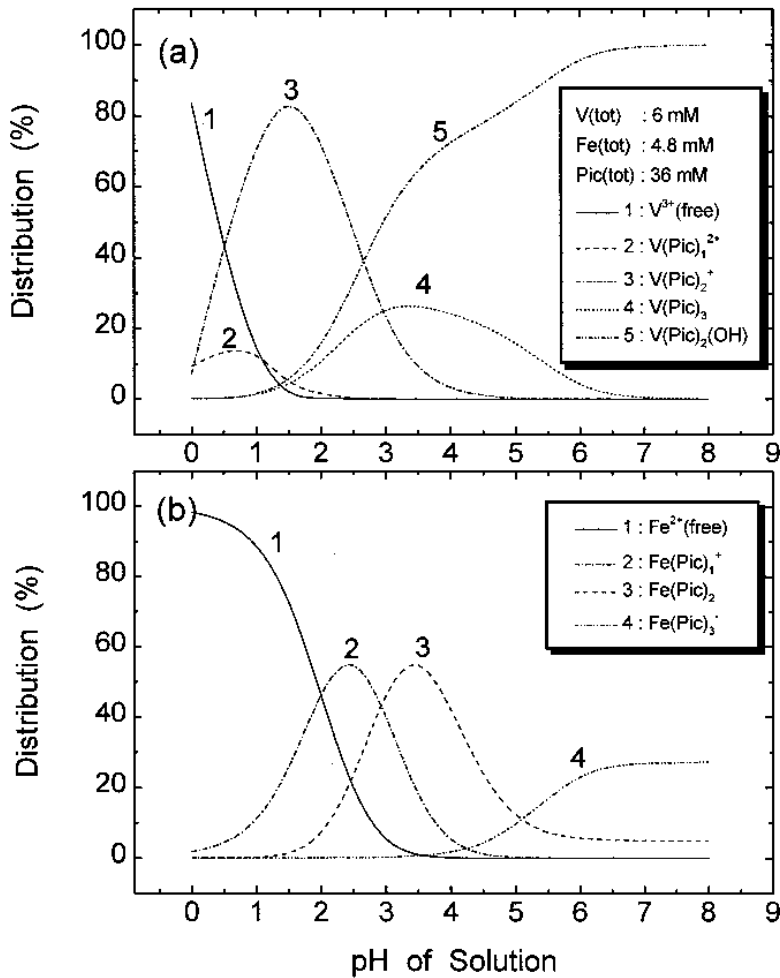


FIG. 3 Distribution diagram of vanadic–picolinate (a), and ferrous–picolinate complexes (b) in the simulated LOMI decontamination solution.  $V^{3+} = 6 \text{ mM}$ ,  $\text{Fe}^{2+} = 4.8 \text{ mM}$ , picolinate = 36 mM.



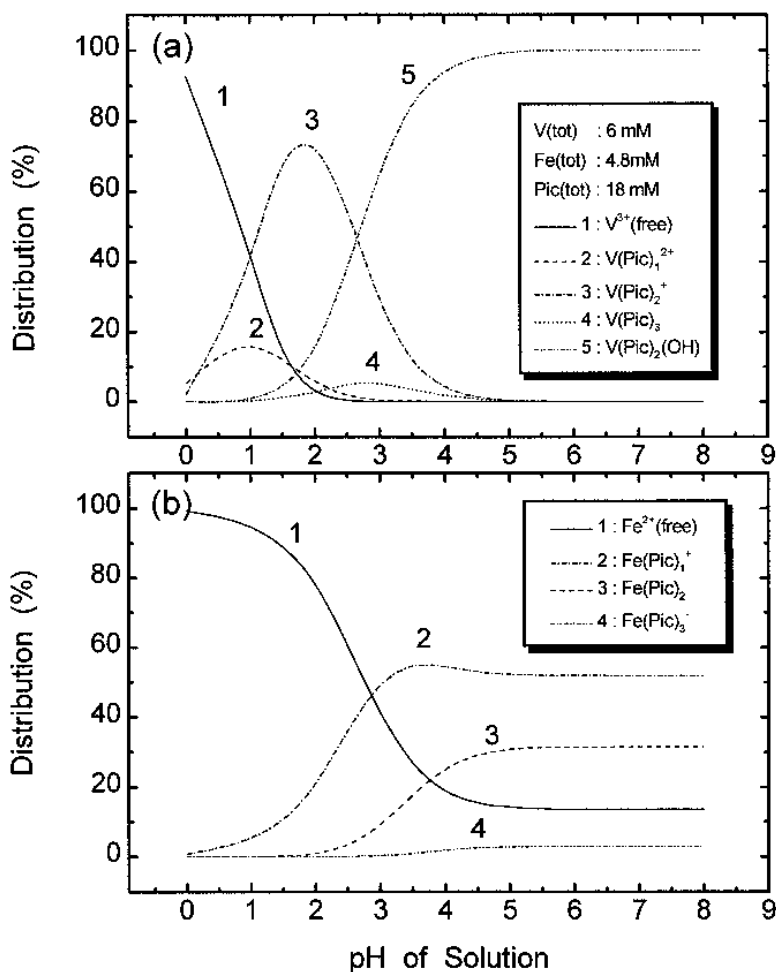


FIG. 4 Distribution diagram of vanadic-picolinate (a), and ferrous-picolinate complexes (b) in the simulated LOMI decontamination solution.  $V^{3+} = 6 \text{ mM}$ ,  $Fe^{2+} = 4.8 \text{ mM}$ , picolinate = 18 mM.

dominantly form positive monovalent  $Fe(II)(Pic)_1^+$  and neutral  $Fe(II)(Pic)_2$  complexes. However, these complexes can be converted to the positively charged forms when hydrogen ions are supplied by forcing the feed to pass through the resin bed filled with the strong acid  $H^+$ -form exchanger. Since both the converted cationic complexes and free cations are easily adsorbed on the cation-exchange resin bed, these species can be easily electrodialyzed to the cathode compartment.

The negatively charged formate and dissociated picolinate present in the solution during the electrodialytic operation will migrate toward the anode compartment, but these ions are rejected at the cation-exchange membrane and remain in the effluent.



### Permeation of Ions through the Nafion Membrane

The simulated decontamination solution contains not only monovalent  $\text{Na}^+$  and  $\text{H}^+$  ions, but also multivalent  $\text{Fe}^{2+}$  and  $\text{V}^{3+}$  ions. Figure 4 shows that the concentration of the  $\text{V}^{\text{III}}(\text{Pic})_2^+$  complex is approximately 70% at pH 1.7. The pH value of the effluent discharged from the electrodialyzer is 1.7. Therefore, it is expected that the buffering effect of excess formates contained inherently in the LOMI waste solution may regulate the level of pH near 1.7, and that most of the vanadium ions are preferentially permeated in the form of the  $\text{V}^{\text{III}}(\text{Pic})_2^+$  complex instead of as  $\text{V}^{3+}$  free ion during the electrodialysis operation.

Figures 5 and 6 show the cumulative normalized concentrations of permeated cations for two different catholytes of 1 N and 0.1 N sulfuric acid. The feed rate is fixed at 2 mL/min, the  $\text{V}/\text{Fe}/\text{Pic}$  ratio is 1:0.8:3 based on  $\text{V} = 6$  mM, and the current density is 80 mA/cm<sup>2</sup>. High concentrations of sulfuric acid extend the life cycle of the catholyte at a fixed volume. As elution continues, the concentrations of cations in the catholyte are enriched. The measured concentrations of vanadium, iron, and sodium in the effluent were 0.18, 0, and 0.81 mM, respectively.

As shown in Fig. 6, the concentration of iron ions (open circles) suddenly decreased and solid particles of iron hydroxide were recovered by the 0.2- $\mu\text{m}$  syringe filters, while vanadium and sodium ions remained in the catholyte.

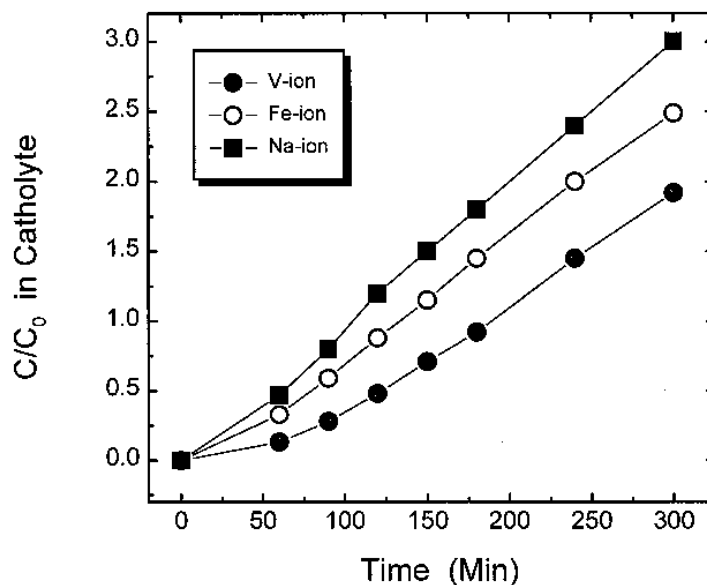


FIG. 5 Variations of cations concentration in catholyte during the electrodialysis of simulated decontamination solution in the resin-filled electrodialyzer. Feed ( $\text{V} = 6$  mM,  $\text{V}/\text{Fe}/\text{Pic} = 1:0.8:3$ ); catholyte = 1 N  $\text{H}_2\text{SO}_4$ ; feed rate = 2 mL/min;  $i = 80$  mA/cm<sup>2</sup>.



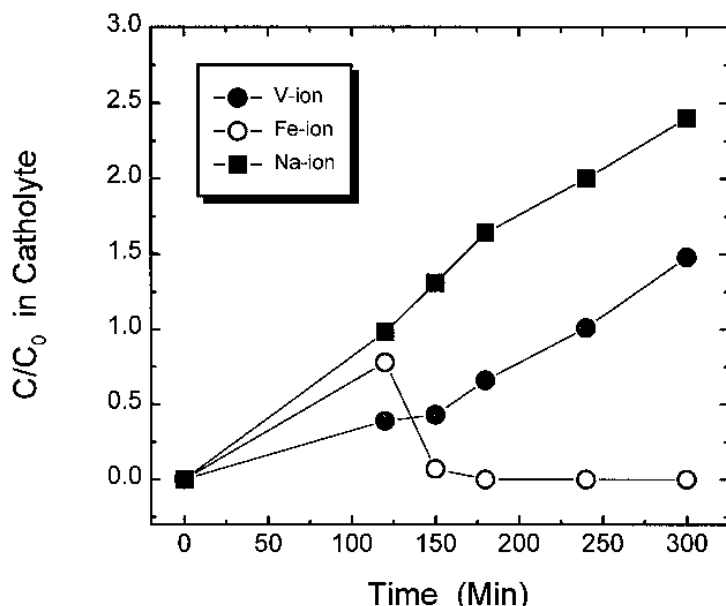


FIG. 6 Variations of cations concentration in catholyte during the electrodialysis of simulated decontamination solution in the resin-filled electrodialyzer. Feed ( $V = 6$  mM,  $V/Fe/Pic = 1:0.8:3$ ); catholyte = 0.1 N  $H_2SO_4$ ; feed rate = 2 mL/min;  $i = 80$  mA/cm $^2$ .

Iron ions were detected in the acidic catholyte before 120 minutes, but they did not exist in the alkaline samples after 150 minutes. The same phenomena were also observed for the catholyte at high concentrations of sulfuric acid (figure not shown).

The pH value of the catholyte was monitored during electrodialysis and is given in Fig. 7. At the initial stage, the pH value was about 1.3. After 180 minutes however, it rapidly increased up to pH 12.3. The increase of catholyte pH is mainly due to the reduction of hydrogen ion to hydrogen gas at the cathode. Iron ions which permeate into the catholyte are converted to hydroxide precipitates at high pH. Therefore, precipitates can be formed by controlling the initial concentration of hydrogen ions in the catholyte and by reducing the hydrogen ions via the formation of hydrogen gas at the cathode. It was also found that the precipitation of iron in the cathode compartment can be self-modulated by shifting the catholyte pH from the acidic to the alkaline state. Therefore, we propose that such a self-controlled precipitation phenomenon of iron ions could be applied to the removal of contaminants from the catholyte without any addition of precipitants.

Cations such as vanadium, iron, and sodium ions permeated from the resin bed (B) to the cathode compartment (C). Here, hydrogen ions in the catholyte were continuously consumed as a result of the electrolytic reduction reaction. However, since the permeated cations replace the number of charges of the



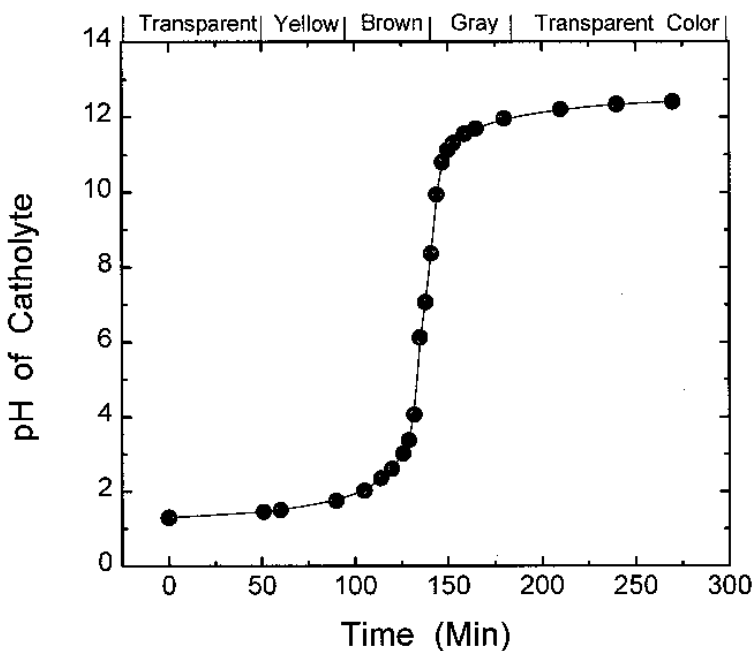


FIG. 7 Variations of catholyte pH during the electrodialysis of simulated decontamination solution in the resin-filled electrodialyzer. Feed ( $V = 6 \text{ mM}$ ,  $V/\text{Fe}/\text{Pic} = 1:0.8:3$ ); catholyte =  $0.1 \text{ N H}_2\text{SO}_4$ ; feed rate =  $2 \text{ mL/min}$ ;  $i = 80 \text{ mA/cm}^2$ .

consumed hydrogen ions, the electroneutrality condition is maintained in the catholyte. Therefore, the pH of the catholyte was changed from an acidic state to a neutral state, probably within about 120 minutes. The catholyte pH increases continuously up to 12 since the water electrolysis reaction occurs in neutral or alkaline medium, and produces hydroxyl ions by Eq. (3), while a part of the permeated cations can be electrolytically reduced at the cathode surface according to Eqs. (4) and (5).

A color change of the catholyte was observed as the pH values increased (see Fig. 7). At pH 2.0 the color of the catholyte was light yellow, and it changed to dark yellow with increasing pH, became brown at pH 2.8, and became dark brown in the 3.0–7.0 pH range. Finally, the color of the catholyte became gray above pH 12. We observed suspended fine particles in the catholyte at this pH region. These observations of color variation confirm that picolimates exist in the catholyte as a result of the electrodialysis of metal ions.

Figure 8 shows the electrical conductivity change of a  $0.1 \text{ N}$  sulfuric acid catholyte. Interestingly, the minimum conductivity of the catholyte was observed near approximately 10 mmho at the greatest pH change region (Fig. 7). At the initial and final stages of the electrodialysis, the electrical conductivity of the catholyte was about 26 mmho. The changes of the electrical conductivity were expected from the molar conductivity difference of each cation in the



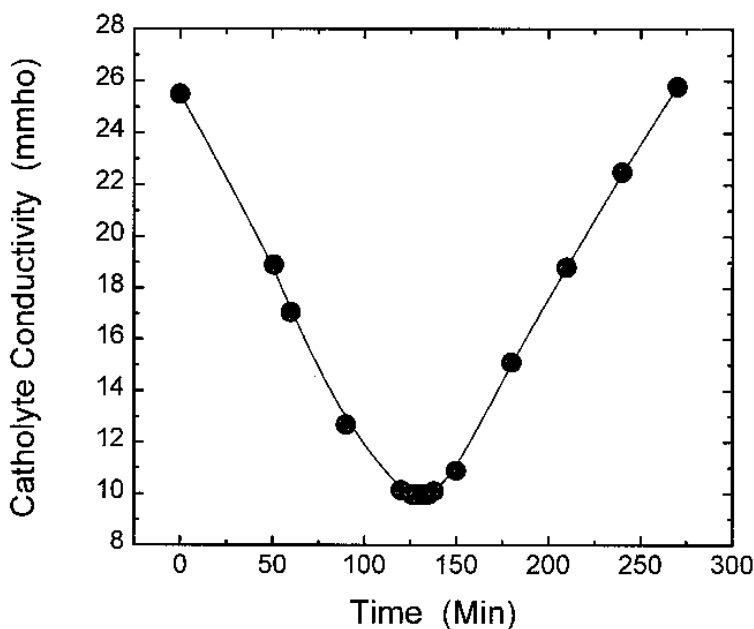


FIG. 8 Variations of catholyte conductivity during the electrodialysis of the simulated decontamination solution in the resin-filled electrodialyzer. Feed ( $V = 6$  mM,  $V/Fe/Pic = 1:0.8:3$ ); catholyte = 0.1 N  $H_2SO_4$ ; feed rate = 2 mL/min;  $i = 80$  mA/cm $^2$ .

catholyte. At an initial stage, hydrogen and sulfate ions moved in the catholyte. The molar conductivity of a hydrogen ion is  $349.82$  cm $^2$ · $\Omega^{-1}$ ·equiv $^{-1}$ , which is 5–9 times greater than those of other cations (19). Hence, the initial electrical conductivity of the catholyte should be high, but this gradually decreases since hydrogen ions at the catholyte are consumed by the cathode reaction. The number of charge carried by hydrogen ions is replaced by those of permeated cations since the electrical neutrality must be satisfied in the electrochemical systems, i.e.,

$$\sum_j z_j C_j = 0 \quad (6)$$

Consequently, the electrical conductivity of the catholyte shows a minimum value at the neutralization point. However, it is believed that the electrical conductivity of the catholyte increases gradually as hydroxyl ions are increasingly produced by the water electrolysis reaction in the alkaline medium. The molar conductivity of hydroxyl ion is  $198$  cm $^2$ · $\Omega^{-1}$ ·equiv $^{-1}$ , which is about 3–5 times greater than those of other anions (19).

### Permeation of Complex Ions

The color change of the catholyte with increasing pH was examined by adding NaOH. Two kinds of catholytes were used: one (actual catholyte) was



generated from electrodialysis of the simulated decontamination solution using 1 N sulfuric acid solution as the catholyte, and the other (artificial catholyte) was prepared as a reference solution having the same composition of the above-mentioned catholyte in the absence of picolinate. As the solution pH increased, the actual catholyte became dark brown in the 3–5 pH range. However, no color variations of the reference solution were observed with increasing pH. Therefore, parts of the picolinate contained in the feed are transported across the cation selective membrane to the cathode compartment in conjunction with the permeated cations.

In Fig. 4 the distribution of species in the simulated LOMI decontamination waste solution with a composition of  $V = 6$  mM and a molar ratio of  $V^{3+}:Fe^{2+}:Pic^-:HCOO^- = 1:0.8:3:10$  shows that most of the vanadium(III)–picolinate complexes exist mainly in the form of  $V^{III}(Pic)_2(OH)$  at pH 4.5 (Fig. 4a), while ferrous–picolinate complexes exist with  $Fe^{II}(Pic)_1^+ = 53\%$ ,  $Fe^{II}(Pic)_2 = 28\%$ ,  $Fe^{2+}$  free ion = 16%, and  $Fe^{II}(Pic)_3^- = 3\%$  at pH 4.5 (Fig. 4b). When the simulated LOMI waste solution of pH 4.5 was electrodialyzed under the conditions of a current density of 80 mA/cm<sup>2</sup> and a feed rate of 2 mL/min, the pH value of the effluent discharged from the electrodialyzer was maintained around 1.6. Therefore, the solution pH within the resin bed is 1.6 or greater. In the 1.7–1.8 pH range, about 70% of vanadium ions exists in the form of the  $V^{III}(Pic)_2^+$  complex, and the fraction of  $Fe^{2+}$  free ions is about 80%. Therefore, it is believed that cations permeated across the membrane will be in the form of the  $V^{III}(Pic)_2^+$  complex and in the form of  $Fe^{2+}$  and  $Na^+$  free ions, respectively. This is consistent with the catholyte color at different pH values (Fig. 7) and the concentration variation of cations in the catholyte (Figs. 5 and 6). In Fig. 6, vanadium ions forming complexes with picolinate ligands remained even in an alkaline solution above pH 12, but ferrous ions were not detected since  $Fe(OH)_3$  precipitates would be formed in an alkaline medium by the oxidation of ferrous ions to ferric ions with air.

In Fig. 9 a plot of the number of charges transferred into the catholyte versus the amount of electricity passed is shown. The filled circle data points are the number of charges transferred by three cationic species, such as  $Na^+$ ,  $Fe^{2+}$ , and  $V(Pic)_2^+$ , across the membrane from the midcompartment to the cathode compartment, and these data points were approximately calculated by using the data values shown in Fig. 5 for each element. The dashed line is the theoretically calculated number of charges based on the electric current. From the data in Fig. 9 and the measured concentrations of sodium, iron, and vanadium in the effluent, the amount of these cations remaining in the resin could be estimated as about 1.74 meq, and the values of the current efficiency for the transport of cations were also calculated. The total value of the current efficiency for the three cations (this value is the ratio of the data point line to the



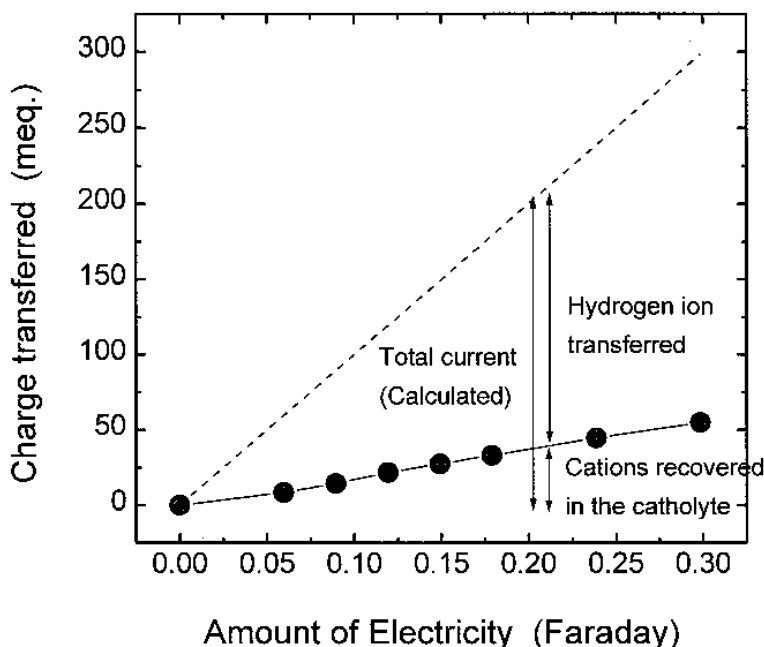


FIG. 9 A plot of the number of charges transferred into the catholyte by cations versus the amount of electricity passed. The filled circles are measured data points, and the dashed line is the theoretically calculated total number of charges.

dashed line) was approximately 18.7%, which was the summation of the individual value of each element. The values of the current efficiency for sodium, iron, and vanadium were 16.3, 1.6, and 0.8%, respectively.

The permeations of anions across cation-exchange membranes can be found in the study by Chum et al. (26) who investigated the permeation behaviors of some carboxylic acids across cation-exchange membrane by the concentration gradient. If these acids are converted to their positively charged cationic forms, then they can permeate through the cation-exchange membrane. Sikdar (27) examined the permeation properties of nine types of carboxylic acids by using a Nafion 117 cation-exchange membrane which was treated with alkaline solution or an acidic form membrane. The diffusion rate of acetic acid through the cation-exchange membrane in acidic form decreases as the ionization degree of carboxylic acid increases, that is to say, as the pH increases. He also studied the permeation behaviors of various amino acids, such as glycine and alanine (28), and found that the permeation tendency of these amino acids across a Nafion membrane depends greatly on the solution pH, and that zwitterionic amino acids give different permeation behaviors with a change of pH. Therefore, it is concluded that anions can permeate through cation selective membranes when they are converted to their posi-



tively charged forms by a change of pH or by other methods such as complexation with cations.

## CONCLUSIONS

The transport of vanadium(III) and iron(II) ions through the Nafion 117 cation-exchange membrane in the presence of picolinic acid was investigated by simulating the equilibrium distribution of ionic species as a function of pH, and by electrodialyzing the simulated waste solution. The mixture of vanadium(III) and iron(II) picolinate complexes was tested by using a resin-filled electrodialyzer.

Based on the distribution calculations of the model reaction systems, it is believed that at pH 1.6 most of vanadium ions exist predominantly in the form of the  $V^{III}(Pic^-)_2^+$  complex, and that this form of complex permeates across the cation-exchange membrane during electrodialysis. Experimental results, including variations in color and the cation concentrations of the catholyte, also support the existence of the vanadium(III)-picolinate complex. Therefore, it is concluded that vanadium ions in the simulated waste solution permeate through the cation-exchange membrane in a form of its picolinate complex.

Iron ions transferred into the catholyte were converted to their hydroxide precipitates at the high pH condition as a result of the reduction of hydrogen ions and the production of  $OH^-$  ions by water electrolysis at the cathode. It was also found that the in-situ precipitation of iron in the electrodialyzer could be self-modulated by shifting the catholyte pH from the acidic to the alkaline state during electrodialysis operation. Therefore, such a self-controlled precipitation phenomenon of iron ions could be applied to the removal of contaminants from the catholyte.

## REFERENCES

1. T. Seto, L. Ehara, R. Komori, A. Yamaguchi, and T. Miwa, *Desalination*, 25, 1-7 (1978).
2. T. C. Huang and I. Y. Yu, *J. Membr. Sci.*, 35, 193-206 (1988).
3. E. Korngold, K. Kock, and H. Strathmann, *Desalination*, 24, 129-139 (1978).
4. S. Itoi, I. Nakamura, and T. Kawahara, *Ibid.*, 32, 383-389 (1980).
5. F. B. Leitz and J. L. Eisenmann, *AICHE Symp. Ser.*, 77, 204-212 (1981).
6. Y. Hara, *Bull. Chem. Soc. Jpn.*, 36, 1373-1376 (1963).
7. G. C. Ganzi, Y. Egozy, A. J. Giuffrida, and A. D. Jha, *Ultrapure Water*, 4(3), 43-50 (1987).
8. T. Xue, R. B. Longwell, and K. Osseo-Asare, *J. Membr. Sci.*, 58, 175-189 (1991).
9. T. Xue and K. Osseo-Asare, *Sep. Sci. Technol.*, 28(4), 1077-1084 (1993).
10. D. Bradbury, M. G. Segal, R. M. Sellers, T. Swan, and C. J. Wood, *EPRI NP-3177*, 1983.
11. C. J. Wood and C. N. Spalaris, *EPRI NP-6433*, 1989.
12. C. J. Wood, *Prog. Nucl. Energy*, 23(1), 35 (1990).
13. R. Soto, *EPRI NP-4240*, 1985.



14. T. Swan, M. G. Segal, W. J. Williams, and M. E. Pick, *EPRI NP-5522M*, 1987.
15. M. S. Davis, *NUREG/CR-3444, Vol. 2*, 1985.
16. D. Bradbury, G. R. Elder, and C. J. Wood, *EPRI NP-7277*, 1991.
17. P. M. Tucker, *Nucl. Eng. Int.*, 38(463), 18–21 (1993).
18. J. S. Newman, *Electrochemical Systems*, Prentice-Hall, Englewood Cliffs, NJ, 1991, p. 61.
19. C. A. J. Bard, *Electrochemical Methods*, Wiley, New York, NY, 1980, p. 67.
20. J. E. Powell and J. W. Ingemanson, *Inorg. Chem.* 7, 2459 (1968).
21. A. M. Lannon, A. G. Lappin, and M. G. Segal, *J. Chem. Soc., Dalton Trans.*, p. 619 (1986).
22. L. G. Sillen and A. E. Martell, *Stability Constants of Metal-Ion Complexes*, Special Publication No. 17. The Chemical Society, Burlington House, London, 1964.
23. J. L. Smee, D. Bradbury, and C. J. Wood, *EPRI NP-7276*, 1991.
24. D. D. Perrin and I. G. Sayce, *Talanta*, 14, 833–842 (1967).
25. N. Ingrı, W. Kakolowicz, L. G. Sillen, and B. Warnquist, *Ibid.*, 14, 1261 (1967).
26. H. L. Chum, D. K. Hauser, and D. W. Sopher, *J. Electrochem. Soc.*, p. 2507 (1983).
27. S. K. Sikdar, *J. Membr. Sci.*, 23, 83 (1985).
28. S. K. Sikdar, *Ibid.*, 24, 59 (1985).

Received by editor May 22, 1998

Revision received October 1998





PAGE 1980 IS BLANK



## **Request Permission or Order Reprints Instantly!**

Interested in copying and sharing this article? In most cases, U.S. Copyright Law requires that you get permission from the article's rightsholder before using copyrighted content.

All information and materials found in this article, including but not limited to text, trademarks, patents, logos, graphics and images (the "Materials"), are the copyrighted works and other forms of intellectual property of Marcel Dekker, Inc., or its licensors. All rights not expressly granted are reserved.

Get permission to lawfully reproduce and distribute the Materials or order reprints quickly and painlessly. Simply click on the "Request Permission/Reprints Here" link below and follow the instructions. Visit the [U.S. Copyright Office](#) for information on Fair Use limitations of U.S. copyright law. Please refer to The Association of American Publishers' (AAP) website for guidelines on [Fair Use in the Classroom](#).

The Materials are for your personal use only and cannot be reformatted, reposted, resold or distributed by electronic means or otherwise without permission from Marcel Dekker, Inc. Marcel Dekker, Inc. grants you the limited right to display the Materials only on your personal computer or personal wireless device, and to copy and download single copies of such Materials provided that any copyright, trademark or other notice appearing on such Materials is also retained by, displayed, copied or downloaded as part of the Materials and is not removed or obscured, and provided you do not edit, modify, alter or enhance the Materials. Please refer to our [Website User Agreement](#) for more details.

**Order now!**

Reprints of this article can also be ordered at  
<http://www.dekker.com/servlet/product/DOI/101081SS100100749>